Original Paper

Kang Liao · Yiping Wu · Fasheng Miao · Linwei Li · Yang Xue

Time-varying reliability analysis of Majiagou landslide based on weakening of hydro-fluctuation belt under wetting-drying cycles

Abstract The impoundment of the Three Gorges Reservoir has a significant impact on the storage area, where the frequent occurrence of reservoir landslides with great harm has attracted much attention. Taking the Majiagou landslide as a case, this study focuses on the hydro-fluctuation belt affected by the reservoir operation. Under the scheduling of reservoir water level, the landslide displacement associated with the hydro-fluctuation belt presents a step-like deformation and the movement behaves as a retrogressive type. The wetting-drying cycles test has been performed to simulate the effects of reservoir water level on the hydro-fluctuation belt. Then, the weakening of soil strength parameters is well characterized by an exponential function model. Considering the continuous weakening of the hydro-fluctuation belt, the time-varying reliability, consistent with the actual landslide zoning, is analyzed under the reservoir operation for 10 years. The results indicate that the migration of seepage field in the landslide is closely related to the scheduling of reservoir water level and lags behind the scheduling. Similarly, the factor of safety varies with the reservoir water level, and the minimum value is obtained when the water drops to the lowest level. With the repeated interaction of reservoir water level on the hydro-fluctuation belt, the most dangerous failure probability of the landslide gradually increases. As a result, the stability of the Majiagou landslide declines from the initial basic stable to the less stable state.

Keywords Reservoir landslides · Hydro-fluctuation belt · Wetting-drying cycles · Time-varying reliability · Failure probability

Introduction

Reservoir landslides are a type of commonly seen geological disaster in the hydropower project area (Han et al. 2018), which are notoriously known due to the wide distribution, strong suddenness, high frequency, and great harm. Reservoir landslides have the potential not only to cause severe casualties and property destruction but also to pose a great damage to hydraulic structures, natural resources, and environmental ecology. For example, the Vajont landslide in Italy on October 9, 1963, and the Qianjiangping landslide in the Three Gorges Reservoir Area (TGRA) of China on July 13, 2003, were both fatal disaster events caused by the scheduling of reservoir water level (Yin et al. 2015; Wolter et al. 2016). Although reservoir landslides have been studied for more than 50 years since the catastrophic Vajont landslide incident occurred, it is still a challenging issue worldwide (Barla and Paronuzzi 2013).

The Three Gorges Hydropower Station on the Yangtze River in China is the world's largest water conservancy project, and the area affected by the massive Three Gorges Reservoir (TGR) is approximately 5.4×10^4 km² (Tang et al. 2019). The reservoir water level fluctuates periodically between 145 and 175 m every year to meet the demands of flood control and power generation, resulting in a hydro-fluctuation belt with a water level difference of 30 m (Wu et al. 2017). The reservoir impoundment has greatly changed the original geological environment of the TGRA and evidently increased the frequency of geological disasters, especially landslides (Song et al. 2018). According to statistics, there are more than 5300 landslides on the shoreline of about 2000 km in the TGRA (Zhang et al. 2018). During the operation of the TGR, the earth mass in the hydro-fluctuation belt undergoes cyclical wetting-drying action, which induces the "fatigue effect" for the earth mass (Deng et al. 2012; Jiao et al. 2014). In this peculiar reservoir environment, the way of the deterioration of strength parameters in the hydro-fluctuation belt and the development of the stability of dangerous landslide caused by the deterioration are two major issues that need to be studied urgently.

The hydro-fluctuation belt undergoes repeated wetting-drying cycles under the cyclical action of reservoir water level, which will lead to changes in composition, microstructure, and mechanical properties of the earth mass (Hussein and Adey 1998; He et al. 2018). Some researchers have combined theories and experiments to study the soil characteristics under wetting-drying cycles (Fleureau et al. 1993; Ng et al. 2009; Bittelli et al. 2012; Zhang et al. 2014; Pasculli et al. 2017). In general, the effects of water on reservoir landslides can be classified into the following two aspects: (1) The periodic scheduling of reservoir water level causes the change of groundwater seepage field, which makes the landslide suffer the floating hydrostatic pressure and hydrodynamic pressure, so that the stability changes dynamically (Wang et al. 2014; Sun et al. 2017; Tang et al. 2019); (2) The repeated wetting-drying alternating process leads to the deterioration of the soil strength, which is likely to stimulate the landslide to develop in an unstable direction (Zhang et al. 2014; Zhang et al. 2015; Liu et al. 2018).

Generally, the sliding zone is considered as the key to control the deformation and evolution of the landslide (Wen et al. 2007; Udvardi et al. 2016; Tomás et al. 2016; Li et al. 2019a). A multitude of researchers have paid close attention to the weakening parameters of the sliding zone through the wetting-drying cycles test, and then evaluated the landslide stability (Penna et al. 2013; Deng et al. 2017). However, the soil in the hydro-fluctuation belt is not only the sliding zone, but more of the sliding mass that interacts with water directly. At present, little attention has been paid to the sliding mass, and works considering the weakening of sliding zone and sliding mass simultaneously under wetting-drying cycles are rarely reported.

The exploration of slope stability has experienced two leaps: the first is from qualitative judgment to quantitative analysis, and the second is from certainty method to uncertainty theory (Liu et al.

2013). Reliability theory is a probability calculation method developed in recent decades, which realizes the second leap of slope stability evaluation and has been widely used in structural engineering (Phoon et al. 2013; Fenton et al. 2016; Li et al. 2017; Juang et al. 2019). Since Crawford and Eden (1967) first introduced reliability theory to slope stability analysis, a growing number of researchers have applied it to slope prevention design and stability evaluation (Shinoda et al. 2006; Low 2008; Zhang et al. 2011; Huang et al. 2017; Gong et al. 2019). Normally, the stability of landslide is analyzed by assuming that the geotechnical properties are fixed or only change over time. However, under natural conditions, the geotechnical properties are variational because of various uncertainties existing in engineering geology, such as those in geotechnical parameters and geological settings (Zhu et al. 2013; Jiang et al. 2018; Gong et al. 2018). That is, the geotechnical properties (cohesion, gravity, internal friction angle, hydraulic conductivity, etc.) are changed within a given range of variation. Therefore, it is of great significance to analyze the landslide stability considering the variation of geotechnical properties.

This study aims to evaluate the time-varying reliability of landslide using the Monte Carlo method. Combined with the existing research results, the Majiagou landslide, which has the representative geometric, material, and kinematic features of reservoir landslides in the TGRA (Gullà et al. 2017; Li et al. 2019b; Tang et al. 2019), is selected as the case study. A series of numerical analyses are conducted to obtain the distribution characteristics of the seepage field under the scheduling of reservoir water level. Subsequently, the time-varying reliability of Majiagou landslide is carried out by considering the weakening of the hydro-fluctuation belt under wetting-drying cycles and the variability of the soil strength parameters (cohesion and internal friction angle). Then, the effects of reservoir operation on the landslide stability are discussed and quantified, which provides insight into the long-term stability of reservoir landslides.

Materials

Geological setting

The Majiagou landslide in the TGRA is located on the left bank of the Zhaxi River, a tributary river of the Yangtze River in Zigui County, Hubei Province (Fig. 1). As shown in Fig. 1b, the Majiagou landslide is opposite to the catastrophic Qianjiangping landslide that has already occurred, separated by the Yangtze River, and the distance between the two landslides is about 10 km (Zhang et al. 2018). In 2003, the TGRA firstly impounded to 135 m. Subsequently, the Majiagou landslide began to show clear deformation signs, and large-scale tensile cracks appeared in the middle and back of the landslide (Ma et al. 2017a). Hence, it was a typical reservoir-induced landslide.

According to the field investigations, the Majiagou landslide is a bedding slope and the slope surface that consists of alternatively gentle and comparatively steep landforms is distributed along the near east-west direction, with an average slope of 15°. The landslide extends over a horizontal distance of 538 m, of which the elevation of the toe is 135 m and the elevation of the crown is 280 m (Fig. 2). The sliding direction that is approximately perpendicular to the Zhaxi River is 291°. The main components of the Majiagou landslide are surficial deposits and sedimentary bedrock. Exploratory trenching showed that the surficial deposits are principally composed of gravelly soil mixed with silty clay; the sedimentary bedrock consists of Jurassic Suining Formation gray sandstone interbedded with purple-red mudstone, which is highly weathered and fractured. Studies have demonstrated that many landslides in the TGRA have occurred in this stratum due to the instability of the Suining Formation (Wen et al. 2004; Fan et al. 2009). Combined with geological survey and drilling technology, the soil-rock interface composed of weathered silty mudstone was determined as the initial sliding surface, and the crack significantly affected by the hydro-fluctuation belt developed into the secondary sliding surface along the interface (Ma et al. 2017b). The calculated sliding mass is 9.68×10^4 m^2, and the deepest part of the sliding zone is 30 m away from the ground, so the overall unstable volume is about 2.52×10^6 m^3. In the light of the volume and the material composition of the landslide, therefore, the Majiagou landslide can be classified as a large-scale colluvial landslide (Hungr et al. 2014).

Monitoring date

Five displacement monitoring stations were arranged at different vertical positions of the landslide (Fig. 2), which could effectively represent the overall deformation of the Majiagou landslide. The time series of the GPS monitoring stations, reservoir water level, and rainfall are presented in Fig. 3.

As shown in Fig. 3, the displacement gradually increased with time and the periodic scheduling of reservoir water level. The G01 at the front of the landslide had a maximum annual deformation of about 183 mm, which implied that the landslide was in a slow deformation stage (Xu et al. 2008). Through analyzing the displacement curves, the deformation of G01, G02, and G03 in the mid-front part of the landslide was similar with each other, showing a step-like characteristic. The step-like deformation occurred in the period of reservoir water drop, and the displacement response was delayed for about 2 months due to the lag effect (Liao et al. 2019). G04 and G05 were located at the back of the landslide, and the step-like characteristic was not observed. This was because there were obvious scour and erosion features in the hydro-fluctuation belt affected by the fluctuation of reservoir water level, which resulted in the deformation of mid-front part in the Majiagou landslide more serious. While the back of the landslide was basically unaffected by the reservoir water level, the displacement was the landslide deformation under natural conditions.

As the reservoir operation progressed, the amplitude of the step-like deformation was gradually decreasing. Taking G01 as an example, the step-like displacements were 106 mm, 91 mm, and 65 mm, respectively. The reason for this phenomenon was that the seepage field, stress field, and structure of the sliding soil in the mid-front part of the landslide had undergone large adjustments after multiple reservoir operations. As a result, when the reservoir water level dropped again, the landslide displacement gradually decreased. Likewise, the displacements of G01–G05 gradually deceased from front to back. The deformation of the mid-front part which was affected by the reservoir water level was much larger than the deformation of the back. It was indicated that the Majiagou landslide was a retrogressive landslide, and the hydro-dynamic pressure and hydrostatic pressure generated by the periodic scheduling of reservoir water level were the main traction forces.
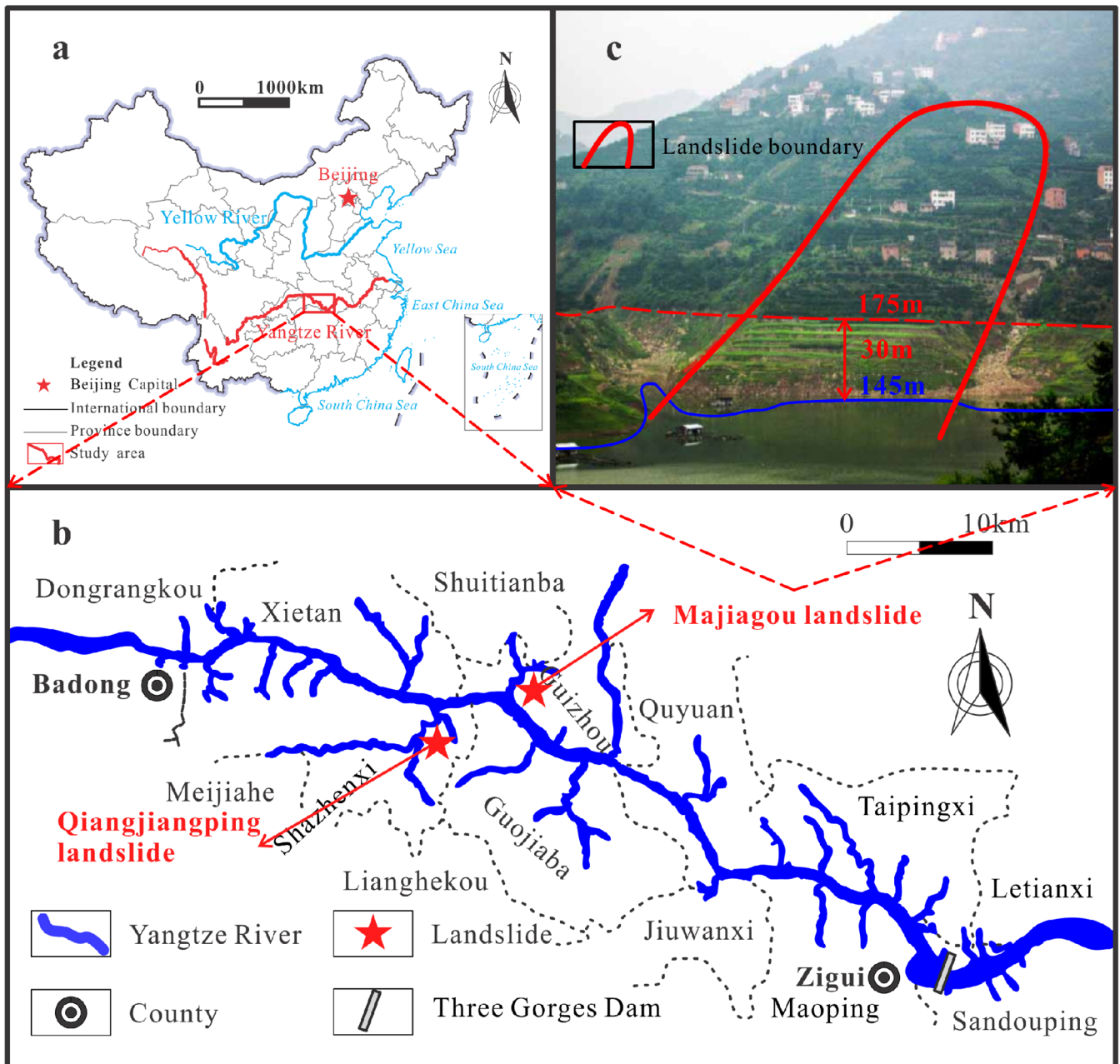
Fig. 1 **a** Location of the study area. **b** location of the Majiagou landslide. **c** geomorphology of the Majiagou landslide (revised from Zhang et al. 2018)

In addition, the time series of rainfall and displacement were also showed in Fig. 3. It could be seen from the figure that the continuous heavy rainfall was mainly concentrated in July to September. During this period and the subsequent period that may be affected by the lag effect, the landslide displacement did not increase significantly, and no step-like characteristic occurred. In particular, the maximum daily rainfall was 121.1 mm in August 2008, which reached the level of heavy rainfall, while the landslide displacement was still unresponsive. Therefore, the landslide deformation had a relatively little correlation with rainfall, which was mainly affected by the fluctuation of reservoir water level in this period.

Wetting-drying cycles test

Since the impoundment of the TGR, the reservoir water level has changed periodically between 145 and 175 m every year on basis of the scheduling arrangement, leading to the formation of a hydro-fluctuation belt with a height of 30 m (Fig. 4), which makes the soil in the belt experience dynamic hydrodynamic pressure and hydrostatic pressure. When the reservoir water level rises, the soil is in a saturated state by the water supply; when the reservoir water level falls, the soil is in an unsaturated state by the water drain (Deng et al. 2012). The soil undergoes continuous wetting-drying cycles, which will lead to the deterioration of mechanical properties. Although the weakening of soil parameters is a gradual
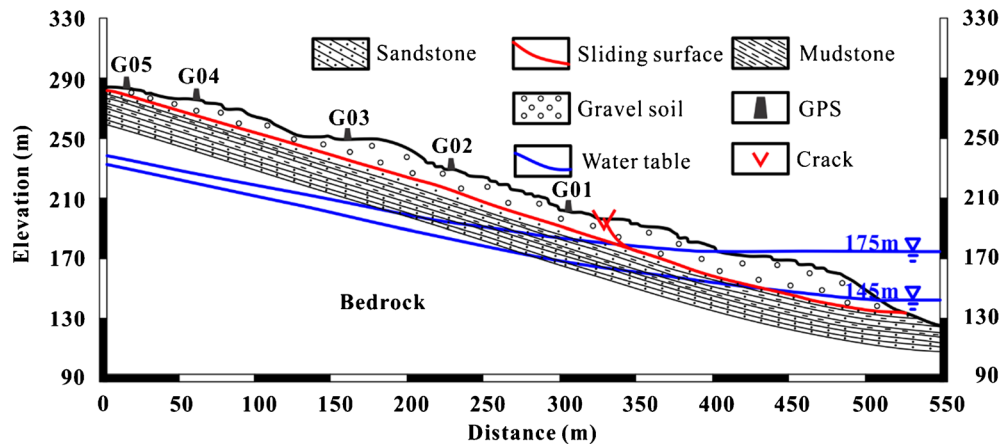
Fig. 2 Schematic geologic cross section of the Majiagou landslide

process and the effects of each weakening may not be conspicuous, the results will accumulate by repeated interaction, resulting in the instability of the reservoir landslides.

For colluvial landslides, the weakening of the soil strength parameters in the hydro-fluctuation belt includes sliding zone and sliding mass. Some researchers have carried out corresponding experimental studies to obtain the laws of soil weakening under wetting-drying cycles (Jiao et al. 2014; Deng et al. 2017; Pasculli et al. 2017). Jiang (2019) studied the weakening of sliding zone under wetting-drying cycles. The samples used in the test program were from the in situ sliding zone of the Majiagou landslide and were divided into six groups, corresponding to the number of wetting-drying cycles. The saturation of the samples was completed by soaking in natural condition, and then, the natural moisture content was reached by drying. Each group contained twelve samples to perform parallel direct shear tests with four normal stresses (50, 100, 150, and 200 kPa). The strain-controlled direct shear apparatus (DYJ-4) was conducted to obtain the strength parameters of the soil at a controlled shear rate of 0.8 mm/min. The results are shown in Table 1.

Deng et al. (2017) selected the representative sliding mass in the hydro-fluctuation belt of the TGRA to simulating the natural soaking and drain process. Seven cycles were arranged in the experiment to explore the relatively stable mechanical state of

the soil under wetting-drying cycles. Meanwhile, in order to match the actual environmental conditions as much as possible, the soaking water was taken from the river near the sampling point. Considering four different normal stresses (100, 200, 300, and 400 kPa), the strength parameters of the soil were performed on a strain-controlled direct shear apparatus (ZJ). The results are shown in Table 2.

Methods

Weakening model
Combined with the existing experimental results and theoretical analysis, the weakening of soil strength parameters under wetting-drying cycles can be good characterized and fitted by the exponential function ω_o as follows:

$$\omega(N) = \omega_o\left(a + be^{-Nd}\right) \tag{1}$$

where ω is the strength parameters of the soil, including cohesion (c) and internal friction angle (ϕ); is the initial value of parameters; N is the number of wetting-drying cycles; a is the residual
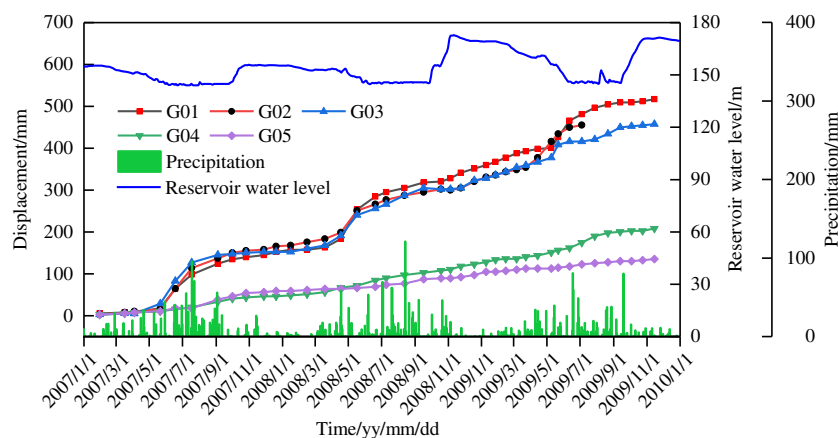

Fig. 3 Monitoring stations displacement, reservoir water level, and daily rainfall over the period February 2007 to November 2009
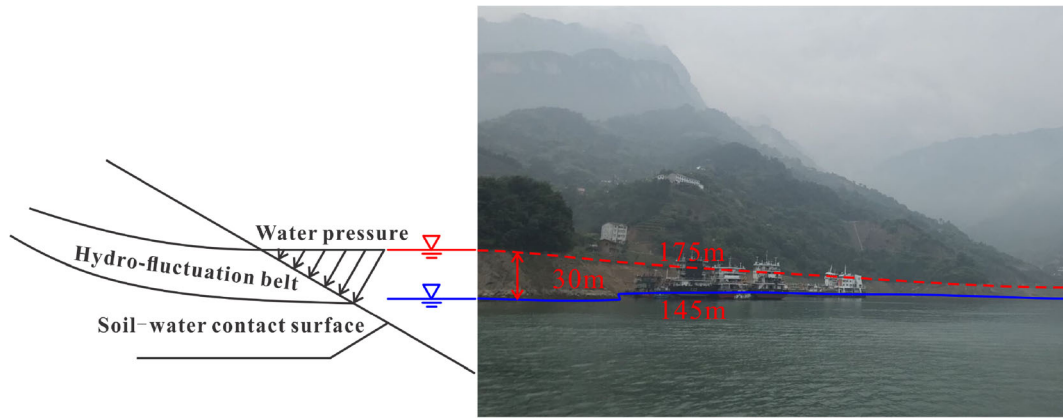
Fig. 4 Typical hydro-fluctuation belt of the reservoir landslide in the TGRA

Table 1 Strength parameters of sliding zone under wetting-drying cycles (Jiang 2019)

Parameters	Time					
	0	1	2	3	4	5
c	27.30	24.17	22.72	21.65	20.88	19.76
ϕ	17.18	15.95	15.19	15.40	14.69	14.72

weakening coefficient; b is the weakening proportionality coefficient; and d is the weakening law coefficient.

It is worth noting that in order to maximize the number of test samples and verify the correctness of the function (Eq. (1)), the strength parameters at $N = 0$ are also fitted. Therefore, $a + b = 1$ is not specified when the parameters are set, so a and b are arbitrary constants.

The weakening function is used to fit the strength parameters (c, ϕ) of the sliding zone, and the coefficients are obtained by using the non-linear fitting method of the Matlab toolbox with 95% confidence bounds. The expression equations are as follows:

$$c = 27.3\left[0.691 + 0.305e^{-0.387N}\right] \tag{2}$$

$$\phi = 17.18\left[0.853 + 0.146e^{-0.639N}\right] \tag{3}$$

Similarly, the weakening function of the sliding mass can be expressed as follows:

$$c = 18.32\left[0.314 + 0.705e^{-0.32N}\right] \tag{4}$$

$$\phi = 19.31\left[0.754 + 0.247e^{-0.234N}\right] \tag{5}$$

Figure 5 shows the degradation curves of the strength parameters (c, ϕ) of sliding zone and sliding mass under wetting-drying cycles. To assess the fitting performance of the model, three statistical indices are introduced (Liao et al. 2019), namely the root mean square error (RMSE), mean absolute percentage error (MAPE), and goodness of fit (R^2).

It can be seen from the results in Table 3 that the RMSE, MAPE, and R^2 of the strength parameters can well reflect the appropriateness of the proposed model, and the fitting accuracy is satisfactory. At the same time, when $N = 0$, the value of $a + b$ is also approximately equal to 1, which is consistent with the actual expectation. Therefore, the given weakening function has a clear physical and mathematical meaning and can well characterize the degradation of the sliding zone and sliding mass under wetting-drying cycles.

Monte Carlo model

In the reliability analysis, the selection of appropriate calculation method is an essential basis for evaluating structural safety, and

Table 2 Strength parameters of sliding mass under wetting-drying cycles (Deng et al. 2017)

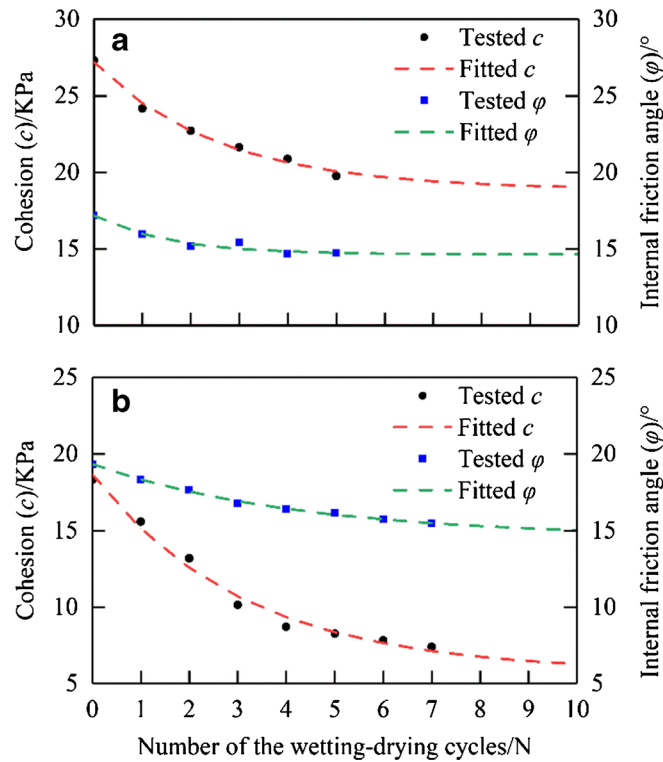| Parameters	Time							
	0	1	2	3	4	5	6	7
c	18.32	15.58	13.21	10.15	8.71	8.27	7.84	7.40
ϕ	19.31	18.33	17.66	16.78	16.39	16.14	15.74	15.46

Fig. 5 Degradation curves of the strength parameters (c, ϕ) of **a** sliding zone and **b** sliding mass under wetting-drying cycles

the plausibility of structural failure is quantified by the failure probability. At present, the probability-based analysis methods can be summarized into two categories: (1) Methods based on a small number of key points sampling, mainly including the first-order reliability method (FORM) and the point estimate method (PEM); (2) Monte Carlo and its derived stochastic simulation methods (Liu et al. 2013). Among these methods, the Monte Carlo method is becoming more and more popular with the rapid advance in computing technology and power. Further, the Monte Carlo method can approach the real solution infinitely, so it can get a more accurate solution than the other methods.

The basic principle of the Monte Carlo method is to first generate samples of random variables, then use these samples as input to obtain samples of the function, and finally count the number of defined failure samples to estimate the failure probability.

For the landslides, it is usually assumed that the random variable X obeys a certain probability distribution, and then generates M sets of random numbers $X_i = (x_{i1}, x_{i2}, \cdots, x_{in})$ satisfying the

Table 3 Fitting accuracy of the strength parameters (c, ϕ) of sliding zone and s-liding mass under wetting-drying cycles

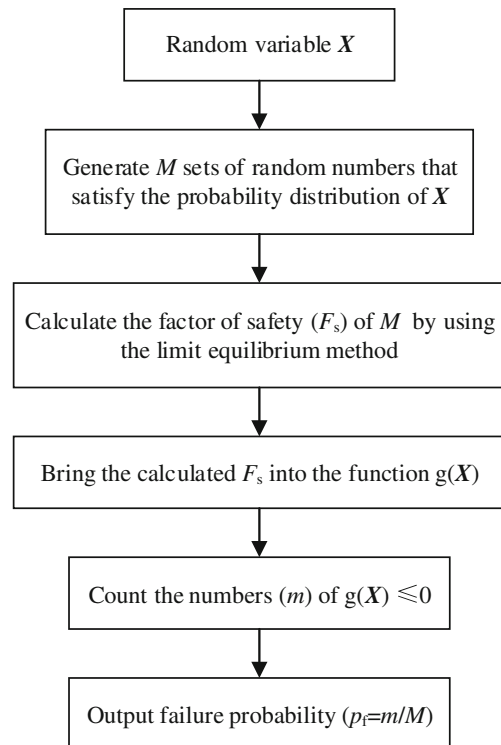| Material	Parameters	RMSE	MAPE	R^2
Sliding zone	c	0.231	0.91	0.991
	ϕ	0.181	0.856	0.955
Sliding mass	c	0.442	3.67	0.987
	ϕ	0.076	0.339	0.996

Fig. 6 Analytical flowchart of the Monte Carlo computation process

Table 4 The statistical characterization values of random variables

Materials	Random variables	Average value	Standard deviation	Coefficient of variation	Probability distribution
Sliding mass	c	18.32	4.03	0.22	Normal distribution
		19.31	4.63	0.24	Normal distribution
Sliding zone	c	27.30	5.46	0.20	Normal distribution
	ϕ	17.18	3.ϕ61	0.21	Normal distribution

probability distribution of X through the random number generator, where $i = 1, 2, \cdots, M$ and n is the number of basic random variables, which can be gravity, cohesion, internal friction angle, hydraulic conductivity, etc.

The generated M sets of random numbers are brought into the function . The $g(X)$ can be calculated as follows:$g(X)$

$$g(X) = F_s(X) - 1 \qquad (6)$$

$$F_s(X) = F_s(x_1, x_2, \cdots x_n) = \frac{R(x_1, x_2, \cdots x_n)}{S(x_1, x_2, \cdots x_n)} \qquad (7)$$

where F_s is the factor of safety, R is the sliding resistance, and S is the sliding force.

The results of the $g(X)$ have three forms, which respectively represent the different states of the landslide:

$$\begin{cases} g(X) > 0, \text{Stable state} \\ g(X) = 0, \text{Limit equilibrium state} \\ g(X) < 0, \text{Failure state} \end{cases} \qquad (8)$$

If there are m sets of random numbers in M to make $g(X) \leq 0$, when M is large enough, the failure probability p_f can be expressed as:

$$p_f = p(g(X_i) \leq 0) = m/M \qquad (9)$$

The basic flow of the computation process is shown in Fig. 6.

In this study, the volume weight and strength parameters of the landslide are important internal factors affecting the calculation results in reliability analysis. In the hydro-fluctuation belt, the periodic fluctuation of reservoir water level leads to the deterioration of strength parameters, but has a relatively small impact on the volume weight. In addition, it is widely accepted that the variability of strength parameters is more obvious than the volume weight, which has a more significant impact on the landslide stability. Therefore, the strength parameters are selected as random variables to establish the ultimate limit function, and the volume weight is considered as a certain value. The F_s of the model is calculated by the Morgenstern-Price method, and the failure occurs if $F_s < 1$ (Eq. (8)). The distribution of the F_s is calculated using the Monte Carlo method. Besides, the number of operations is set to 5000 to improve the reliability of the calculation (Eq. (9)).

Furthermore, it is roughly assumed that one wetting-drying cycle corresponds to one reservoir operation. Hence, according to the weakening model obtained in Eqs. (2)–(5), the 10 wetting-drying cycles strength parameters of sliding zone and sliding mass predicted by the fitting function are selected to correspond to 10 reservoir operations. Taking the initial strength parameters as an example, the statistical characterization values of random variables are shown in Table 4.
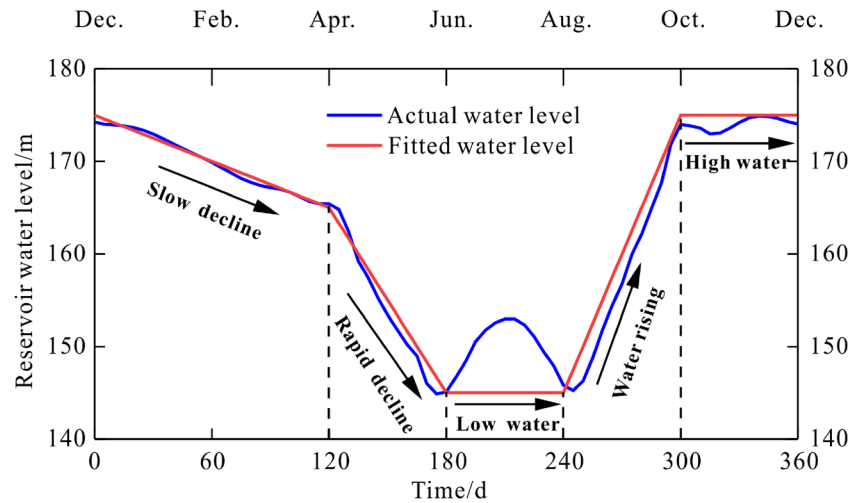
Numerical calculation model

Simulation of seepage field
Based on the geological model (Fig. 2), monitoring data and geotechnical properties of the Majiagou landslide, a two-
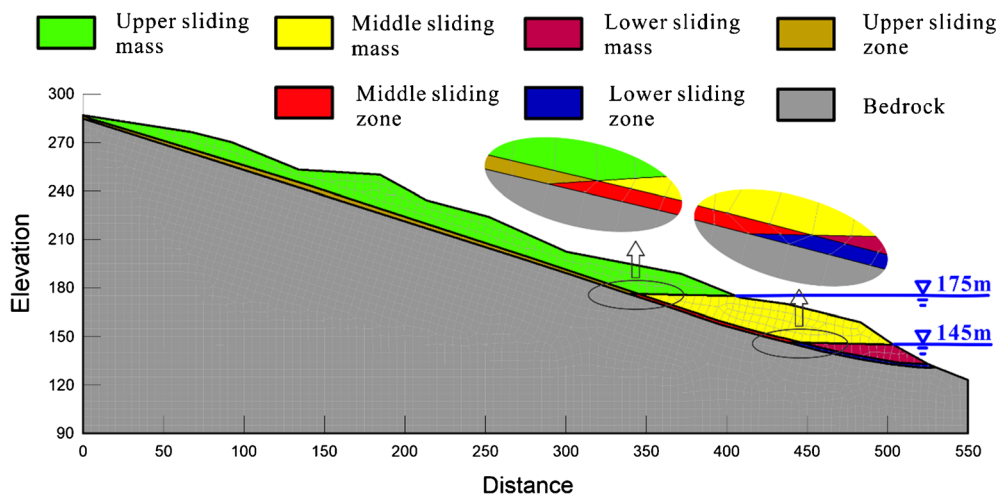
Fig. 7 Seepage field model of the Majiagou landslide

Fig. 8 The scheduling curve of reservoir water level for 1 year

dimensional finite element model with a length of 550 m and a height of 287 m (Fig. 7) is established to simulate the seepage field of the landslide. The established model composed of quadrilateral cells and small amounts of trilateral transitional cells is partitioned into 2779 grid cells and 2892 nodes. The boundary conditions of the landslide model, which are simulated in SEEP/W of the GeoStudio software, are arranged as follows: (1) The leading edge of the sliding mass is determined to be the boundary of the varying head, which changes with the scheduling of reservoir water level. (2) The groundwater level at the trailing edge of the landslide is basically not affected by the reservoir operation according to the monitoring data, so the trailing edge of the landslide is determined to be the boundary of the constant water head with an elevation of about 232 m. (3) The bottom of the model is the boundary of water proof. Besides, the volumetric water content function adopted here is for a silty clay material with a saturated water content, and the hydraulic conductivity function is estimated using the Van Genuchten method with a saturated hydraulic conductivity.

Meanwhile, in order to simulate the scheduling of reservoir water level in the TGRA more realistically, a representative scheduling curve is designed as the input of the varying head (Tang et al. 2019). Further, a series of linear functions are used to fit the fluctuation of reservoir water level and eliminate the accidental errors caused by monitoring (Fig. 8). The designed functions are as follows:

$$H(t) = \begin{cases} 175 - t/12, & t \in (0, 120d) \\ 205 - t/3, & t \in (120, 180d) \\ 145, & t \in (180, 240d) \\ 25 + t/2, & t \in (240, 300d) \\ 175, & t \in (300, 360d) \end{cases} \quad (10)$$

As described in Fig. 8, the scheduling of reservoir water level can be divided into 5 phases: slow decline period (January–April, 0–120 days), rapid decline period (April–June, 120–180 days), low water period (June–August, 180–240 days), water rising period (August–October, 240–300 days), and high water period (October–December, 300–360 days). The designed reservoir water level is basically consistent with the actual level (Table 5), but there are some discrepancies in the low water period. The reason behind this result is that the June to August of each year is usually the seasonal rainfall period of the TGRA, so the reservoir water level will be adjusted to meet the specific demands. In addition, vessel traffic and power generation will also cause the fluctuation of reservoir water level tentatively. Hence, the reservoir water level during this period has great uncertainty and is taken as the minimum level of 145 m without considering other external factors.
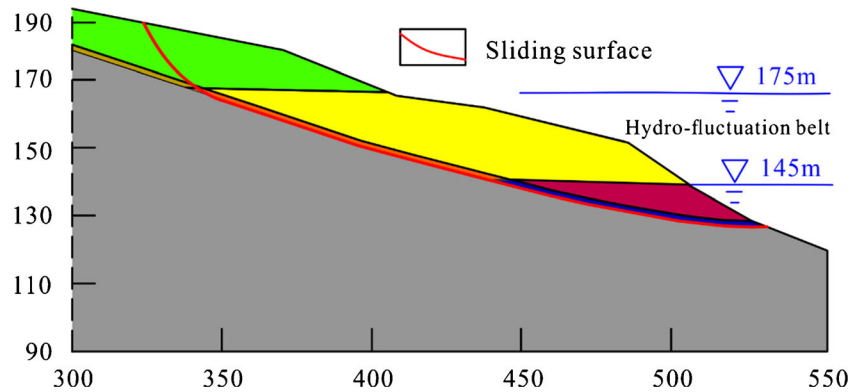
Stability analysis

In the previous studies on landslide stability, the sliding zone and the sliding mass were usually considered as two parts, each of which was assigned the same parameters. Differently, this model divides the landslide into seven areas considering the influence of the hydro-fluctuation belt (Fig. 7), namely, upper sliding mass, middle sliding mass, lower sliding mass, upper sliding zone, middle sliding zone, lower sliding zone, and bedrock. The lower sliding mass and lower sliding zone are saturated because they are located below the groundwater level for a long time. The middle sliding mass and middle sliding zone are located in the hydro-fluctuation, which are continuously affected by the reservoir water level. The upper sliding mass and upper sliding zone are in a natural state.

Table 5 Fitting accuracy of measured and modeled time series of the reservoir water level

Period	Slow decline	Rapid decline	Low water	Water rising	High water
RMSE	0.36	1.33	-	2.66	1.12

Fig. 9 The geotechnical model of the landslide for stability analysis

The Majiagou landslide appeared large-scale cracks since the TGRA was impounded. The site-specific investigation showed that crack, which was directly affected by the hydro-fluctuation belt, developed along the initial soil-rock interface and reached approximately 80 m in length and 0.1 to 0.5 m in width. Meanwhile, the monitoring data also demonstrated that the deformation of the landslide in the hydro-fluctuation belt increased observably under the reservoir operation. These signs have contributed to the formation of a secondary sliding surface in the affected area (Ma et al. 2017b). Therefore, the secondary sliding surface that is significantly affected by the fluctuation of reservoir water level is selected for stability analysis. The geotechnical model used for stability analysis is shown in Fig. 9, and the basic calculation parameters of the model are shown in Table 6 (Ma et al. 2017a; Hu et al. 2019).

Results

Transient seepage field

The seepage field in the landslide is simulated using the module SEEP/W in the GeoStudio. Firstly, the steady seepage field when the reservoir water level is 175 m is selected as the beginning of the analysis (0 day), and the upper limit of the hydro-fluctuation belt is determined. Likewise, the lower limit of the hydro-fluctuation belt is determined when the reservoir water level is 145 m. Then, the changes of the seepage field with the rise and fall of reservoir water level are calculated. Taking a reservoir operation cycle (360 days) as an example, the results of the saturation line at different phases can be summarized as follows:

1. Water decline period (January–June, 0–180 days): According to different operation conditions, the reservoir water level drops from high water level to low water level at different rates. Generally, the slow decline period is from January to April (0–120 days), and the reservoir water level drops at an average speed of 0.083 m/day. The rapid decline period is from April to June (120–180 days), and the reservoir water level drops at an average speed of 0.33 m/day. As shown in Fig. 10a, the saturation line is convex, which means the groundwater level replenishes the reservoir water level, causing the groundwater level to drop continuously. Meanwhile, the decline rate of groundwater in the rapid decline period is quicker than that in the slow decline period.

2. Water rising period (August–October, 240–300 days): The reservoir water level rises at an average speed of 0.5 m/day from 145 m. It can be seen from Fig. 10b that the saturation line of sliding mass rises in a concave shape as the continuous rise of reservoir water level. During this phase, the external reservoir water level and the internal groundwater level of the model generate a head difference, so the reservoir water level supplements the groundwater level. At the same time, the saturation line shows a concave shape, which implies that there is a certain lag between the seepage response inside the landslide and the fluctuation of reservoir water level.

3. Water stable period (June–August, 180–240 days; October–December, 300–360 days): From June to August (180–240 days), the reservoir water is at a low level of 145 m (Fig. 10a); from October to December (300–360 days), the reservoir water is at a high level of 175 m (Fig. 10b). When the reservoir water level maintains stable, the groundwater level will continue to adjust due to the lag effect, and eventually reach a smooth state. It is worth noting that there may be many cracks, joints, and faults inside the landslide, so the time to reach the smooth state will be much shorter than the results of numerical simulation.

Time-varying reliability

Prior to performing the time-varying reliability analysis, the F_s within a scheduling period of reservoir water level is calculated to study the effects of dynamic seepage on the landslide stability, and the results are shown in Fig. 11.

It can be seen from Fig. 11 that the F_s is closely related to the scheduling of reservoir water level. When the reservoir water level drops, the F_s decreases accordingly, and reaches a minimum value of 1.17 at 180 days. At the same time, the change of the F_s is positively correlated with the decline rate of reservoir water level. Similarly, the F_s increases as the reservoir water level rises. When the reservoir water level maintains stable, the F_s will change slightly due to the lag effect, which reflects the adjustments made by landslide body to the fluctuation of reservoir water level. Therefore, in order to effectively improve the reliability calculation efficiency, the moment of the most dangerous failure probability that the

Table 6 The calculation parameters of the finite element model

Materials	Unit weight (kN/m³)		Cohesion (kPa)		Internal friction angel (°)		Hydraulic conductivity (m/day)	Saturated water content (%)	Residual water content (%)
	Natural	Saturated	Natural	Saturated	Natural	Saturated			
Sliding mass	21.14	22.05	18.32	16.21	19.31	17.68	1.05	43	3
Sliding zone	21.84	22.52	27.30	25.15	17.18	15.26	0.62	35	15
Bedrock	25.20	-	3000	-	35	-	8.64E−4	24	0

reservoir water level drops to the lowest level is selected for calculation.

The module SLOPE/W, which employs the seepage field results from the SEEP/W, is adopted in the time-varying reliability model of the landslide. Considering the reservoir operation and the weakening of the hydro-fluctuation belt for 10 years, the calculation results of time-varying reliability are shown in Fig. 12.

As shown in Fig. 12, the failure probability of the landslide without experiencing wetting-drying cycles is 11.78%. According to the classification of failure probability and stability state shown in Table 7 (Zhang et al. 1994), the failure probability of this value indicates that the landslide is basic stable. With the extension of the reservoir operation period, the number of wetting-drying cycles in the hydro-fluctuation belt is increasing, and the failure probability gradually rises. After the third scheduling cycles of reservoir water level, the state of the landslide changes from basic stable to less stable. In the subsequent analysis, since the effect of reservoir water level on the landslide tends to be gentle and the deterioration of strength parameters becomes slight over time, the failure probability shows a relatively stable trend. After 10-year scheduling of reservoir water level, the failure probability of the landslide eventually reaches 37.33%, which is an increase of 25.55% compared with the beginning, and the stability state of the Majiagou landslide declines from the initial basic stable to the less stable. Combined with the field investigations, there were multiple expansion cracks in the mid-front part of the Majiagou landslide after several processes of the reservoir operation (Zhang et al. 2018), which were in good agreements with the calculation results.

Discussion

Weakening of sliding mass

In this study, the limit equilibrium method is performed to analyze the stability of the Majiagou landslide considering the weakening of the hydro-fluctuation belt. But, according to the Morgenstern-Price method, it seems that the weakening of the sliding mass has no effect on the stability due to the specified sliding surface. In order to further explore the effects of the weakening of the sliding zone and sliding mass synchronously on the stability of the landslide, we try to search the sliding surface automatically instead of fully specified. Coincidentally, the most dangerous sliding surface obtained through automatic search is consistent with the specified one. The intrinsic reason behind this result is that the strength of the sliding zone is always less than that of the sliding mass under wetting-drying cycles. Hence, the sliding surface specified in the sliding zone represents the most dangerous sliding surface.

However, this kind of coincidence does not apply to all reservoir landslides, especially for colluvial landslides when the strength of the sliding mass is less than that of the sliding zone under wetting-drying cycles. In this case, the position of the most dangerous sliding surface may change, and the surface will partially pass through the previous sliding mass. As a result, the failure probability of the landslide will increase compared with the specified sliding surface. For example, if after 10 cycles, the ϕ of the sliding mass degenerates to 10°, which is less than 14.65° of the sliding zone. The most dangerous sliding surface obtained here is no longer the one previously specified (Fig. 13). Furthermore, the failure probability of the landslide has increased to 51.11% with the new sliding surface compared with the previous 37.33%. Such
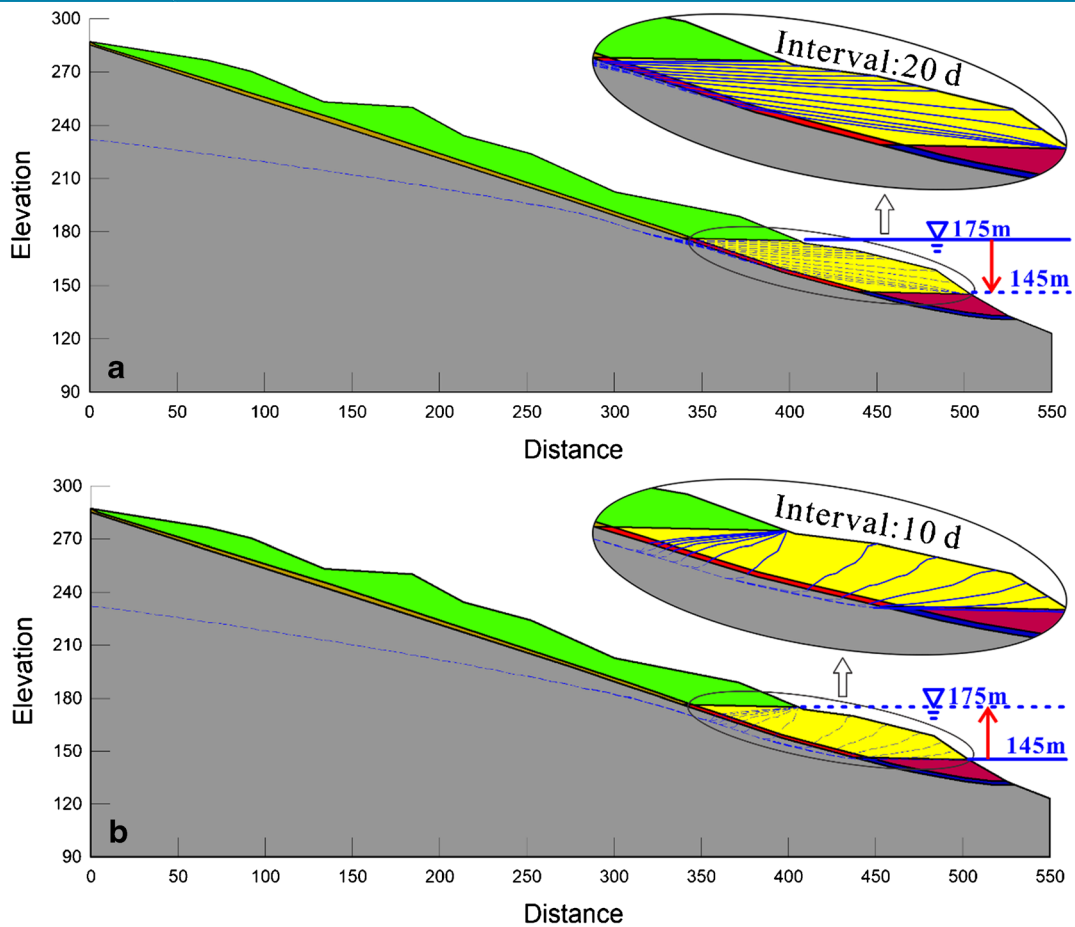
Fig. 10 Saturation line at different times with reservoir water level at **a** 175–145 m and **b** 145–175 m

results demonstrate that the weakening of the sliding mass will also adversely affect the stability of the landslide under certain conditions, which should be paid enough attention as well, especially for the long-term stability study of the reservoir landslides.

Weakening model

Based on wetting-drying cycles test in the materials, this study adopts the proposed weakening model to outline the strength parameters of sliding zone and sliding mass, showing a high accuracy. But due to the differences in test conditions, time and space, there are certain accidental errors in the value of the parameters. At the same time, the weakening of soil under wetting-drying cycles is a cumulative process, which is the result of long-term and multi-frequency action. The number of cycles selected in the test and the fitted curves of the model can, within limits, characterize the degradation of soil strength parameters, but it cannot reflect the weakening process throughout. Therefore, in the purpose of realizing the weakening expression of soil under wetting-drying cycles for a long period, further verification test is needed.
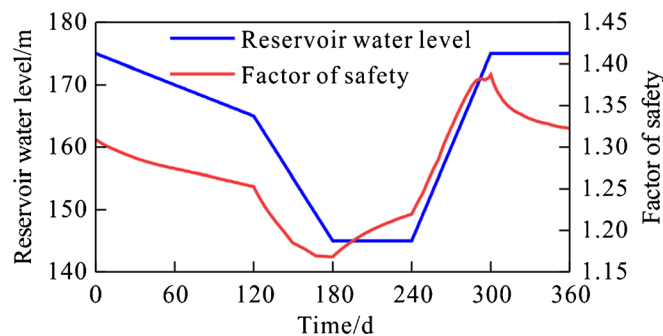

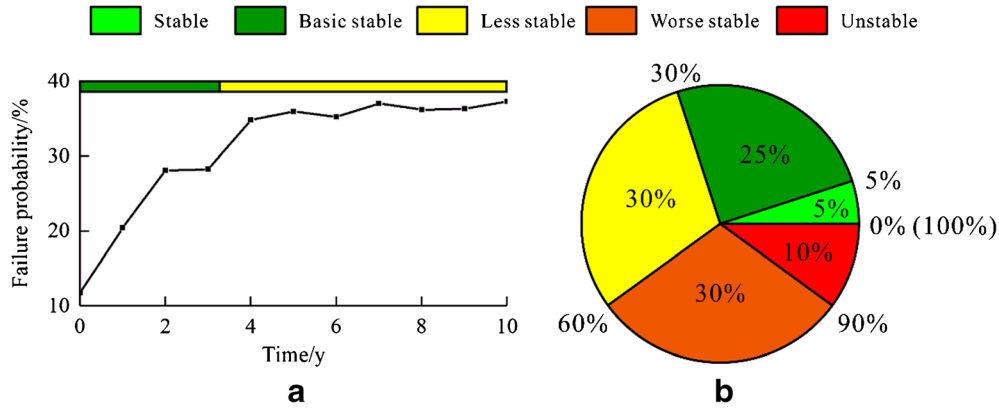**Fig. 11** Relationship diagram of reservoir water level and F_s

Fig. 12 a The failure probability of landslide at different scheduling periods of reservoir water level. **b** Comparison diagram of failure probability and stability

Table 7 The classification table of failure probability and the slope stability state

Stability state	Stable	Basic stable	Less stable	Worse stable	Unstable
Failure probability	0–5%	5–30%	30–60%	60–90%	90–100%

Deformation history

The Majiagou landslide showed clear deformation signs after the impoundment of the TGRA, posing a huge threat to the surrounding environment. In order to prevent the recurrence of the disaster like Qianjiangping landslide, a series of treatments were carried out on the landslide in 2006, including monitoring measures, anti-slide piles, and drainage systems. However, these efforts did not control the deformation effectively. For this reason, two more test piles were constructed on the landslide in 2011, which played a positive role in blocking the deformation (Zhang et al. 2018). Therefore, the monitoring date from 2007 to 2009 when the anti-slide piles were inoperative was selected for analysis. Although the data was limited, it clearly reflected the basic laws of landslide deformation under the reservoir operation. For further analyzing the deformation and evolution characteristics of the Majiagou landslide, the latest monitoring data should be supplemented to study the landslide-stabilizing pile system.

Conclusions

The periodic scheduling of reservoir water level in the TGRA has formed a distinct hydro-fluctuation belt, which adversely affects the stability of reservoir landslides. Majiagou landslide, a representative reservoir landslide in the TGRA, demonstrates a hydro-fluctuation belt under the reservoir operation as well. Combined with the monitoring data and kinematics analysis, the landslide shows an apparent step-like deformation and behaves a retrogressive characteristic due to the influence of reservoir water on the hydro-fluctuation belt.

The soil in the hydro-fluctuation belt undergoes continuous fluctuation of reservoir water level, resulting in the weakening of strength parameters. An exponential function model that has a clear physical and mathematical meaning is conducted to fit the weakening of soil strength parameters under wetting-drying cycles. The fitting achieves satisfactory results, and the proposed weakening model has the potential for broad application to analyze the other reservoir landslides with a hydro-fluctuation belt.
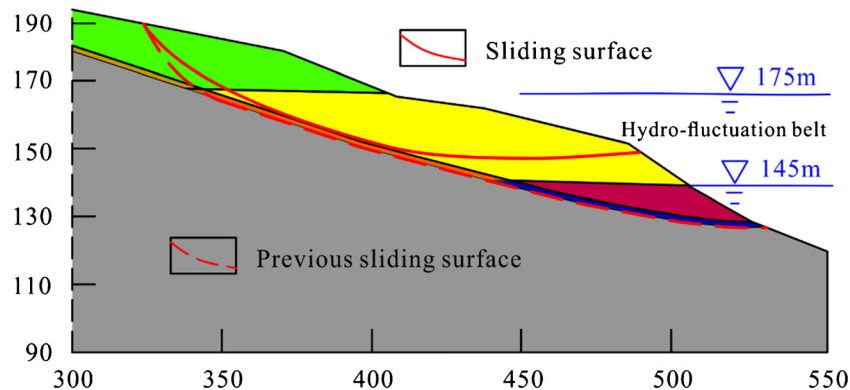

Fig. 13 New geotechnical model obtained via automatic search for stability analysis

The seepage field of the landslide is analyzed through the numerical model which is divided into 7 areas considering the weakening of the sliding zone and the sliding mass in the hydro-fluctuation belt simultaneously. The saturation line is dominated by the fluctuation of reservoir water level, and appears a concave shape when the reservoir level rises and a convex shape when it drops. Besides, the migration of the saturation line lags behind the scheduling of the reservoir water level.

The F_s of the landslide varies with the scheduling of reservoir water level, and the minimum F_s is obtained when the water drops to the lowest level. With the continuous weakening of the sliding zone and sliding mass in the hydro-fluctuation belt, the failure probability increases from the initial 11.78 to 33.73%, and the landslide changes from a basic stable state to a less stable state. Therefore, the management of risk mitigation turns out to be a major priority and adequate countermeasures should be taken to stabilize the landslide.

Acknowledgments

Funding information

References

Barla G, Paronuzzi P (2013) The 1963 Vajont landslide: 50th anniversary. Rock Mech Rock Eng 46(6):1267–1270

Bittelli M, Valentino R, Salvatorelli F, Rossi Pisa P (2012) Monitoring soil-water and displacement conditions leading to landslide occurrence in partially saturated clays. Geomorphology 173:161–173

Crawford CB, Eden WJ (1967) Stability of natural slopes in sensitive clay. J Soil Mech Found Div 93:419–436

Deng HF, Li JL, Zhu M, Wang KW, Wang LH, Deng CJ (2012) Experimental research on strength deterioration rules of sandstone under "saturation-air dry" circulation function. Rock Soil Mech 33:3306–3312 (In Chinese)

Deng HF, Xiao Y, Fang JC, Zhang HB, Wang CXJ, Cao Y (2017) Shear strength degradation and slope stability of soils at hydro-fluctuation belt of river bank slope during drying-wetting cycle. Rock Soil Mech 38(9):2629–2638 (In Chinese)

Fan XM, Xu Q, Zhang ZY, Meng DS, Tang R (2009) The genetic mechanism of a translational landslide. Bull Eng Geol Environ 68(2):231–244

Fenton GA, Naghibi F, Griffiths DV (2016) On a unified theory for reliability-based geotechnical design. Comput Geotech 78:110–122

Fleureau JM, Kheirbek-Saoud S, Soemitro R, Taibi S (1993) Behavior of clayey soils on drying-wetting paths. Can Geotech J 30(2):287–296

Gong W, Juang CH, Martin JR, Tang H, Wang Q, Huang H (2018) Probabilistic analysis of tunnel longitudinal performance based upon conditional random field simulation of soil properties. Tunn Undergr Sp Technol 73:1–14

Gong W, Tang H, Wang H, Wang X, Juang CH (2019) Probabilistic analysis and design of stabilizing piles in slope considering stratigraphic uncertainty. Eng Geol 259:105162

Gullà G, Peduto D, Borrelli L, Antronico L, Fornaro G (2017) Geometric and kinematic characterization of landslides affecting urban areas: the Lungro case study (Calabria, Southern Italy). Landslides 14:171–188

Han B, Tong B, Yan J, Yin C, Chen L, Li D (2018) The monitoring-based analysis on deformation-controlling factors and slope stability of reservoir landslide: Hongyanzi landslide in the southwest of China. Geofluids:1–14

He P, Li S-C, Xiao J, Zhang Q-Q, Xu F, Zhang J (2018) Shallow sliding failure prediction model of expansive soil slope based on Gaussian process theory and its engineering application. KSCE J Civ Eng 22(5):1709–1719

Hu X, He C, Zhou C, Xu C, Zhang H, Wang Q, Wu S (2019) Model test and numerical analysis on the deformation and stability of a landslide subjected to reservoir filling. Geofluids 2019:1–15

Huang J, Fenton G, Griffiths DV, Li D, Zhou C (2017) On the efficient estimation of small failure probability in slopes. Landslides 14(2):491–498

Hungr O, Leroueil S, Picarelli L (2014) The Varnes classification of landslide types, an update. Landslides 11(2):167–194

Hussein J, Adey MA (1998) Changes in microstructure, voids and b-fabric of surface samples of a Vertisol caused by wet/dry cycles. Geoderma 85(1):63–82

Jiang QQ (2019) Study on the reactivation mechanism and stability of typical ancient landslide in the three gorges reservoir area. Doctoral dissertation. University of Chinese Academy of Sciences, China (In Chinese)

Jiang SH, Huang J, Huang F, Yang J, Yao C, Zhou C (2018) Modelling of spatial variability of soil undrained shear strength by conditional random fields for slope reliability analysis. Appl Math Model 63:374–389

Jiao YY, Song L, Tang HM, Li YA (2014) Material weakening of slip zone soils induced by water level fluctuation in the ancient landslides of Three Gorges reservoir. Adv Mater Sci Eng 2014:1–9

Juang CH, Zhang J, Shen MF, Hu JZ (2019) Probabilistic methods for unified treatment of geotechnical and geological uncertainties in a geotechnical analysis. Eng Geol 249:148–161

Li DQ, Peng X, Khoshnevisan S, Juang CH (2017) Calibration of resistance factor for design of pile foundations considering feasibility robustness. Comput Geotech 81:229–238

Li C, Tang HM, Han DW, Zou ZX (2019a) Exploration of the creep properties of undisturbed shear zone soil of the Huangtupo landslide. Bull Eng Geol Environ 78(2):1237–1248

Li CD, Fu ZY, Wang Y, Tang HM, Yan JF, Gong WP, Yao WM, Criss RE (2019b) Susceptibility of reservoir-induced landslides and strategies for increasing the slope stability in the Three Gorges Reservoir Area: Zigui Basin as an example. Eng Geol 261:105279

Liao K, Wu Y, Miao F, Li L, Xue Y (2019) Using a kernel extreme learning machine with grey wolf optimization to predict the displacement of step-like landslide. Bull Eng Geol Environ:1–13

Liu X, Tang HM, Xiong CR (2013) Patterns, problems, and development trends of analysis methods for slope dynamic reliability. Rock Soil Mech 34(5):1217–1234 (in Chinese)

Liu XR, Jin MH, Li DJ, Zhang L (2018) Strength deterioration of a Shaly sandstone under dry-wet cycles: a case study from the Three Gorges Reservoir in China. Bull Eng Geol Environ 77(4):1607–1621

Low BK (2008) Efficient probabilistic algorithm illustrated for a rock slope. Rock Mech Rock Eng 41(5):715–734

Ma JW, Tang HM, Hu XL, Bobet A, Yong R, Ez Eldin MAM (2017a) Model testing of the spatial-temporal evolution of a landslide failure. B Eng Geol Environ 76:323–339

Ma JW, Tang HM, Hu XL, Bobet A, Zhang M, Zhu TW, Song YJ, Ez Eldin MAM (2017b) Identification of causal factors for the Majiagou landslide using modern data mining methods. Landslides 14:311–322

Ng CWW, Xu J, Yung SY (2009) Effects of wetting-drying and stress ratio on anisotropic stiffness of an unsaturated soil at very small strains. Can Geotech J 46(9):1062–1076

Pasculli A, Sciarra N, Esposito L, Esposito AW (2017) Effects of wetting and drying cycles on mechanical properties of pyroclastic soils. Catena 156:113–123

Penna D, Brocca L, Borga M, Fontana GD (2013) Soil moisture temporal stability at different depths on two alpine hillslopes during wet and dry periods. J Hydrol 477:55–71

Phoon KK, Ching J, Chen JR (2013) Performance of reliability-based design code formats for foundations in layered soils. Comput Struct 126:100–106

Shinoda M, Horii K, Yonezawa T, Tateyama M, Koseki J (2006) Reliability-based seismic deformation analysis of reinforced soil slopes. Soils Found 46(4):477–490

Song K, Wang FW, Yi QL, Lu SQ (2018) Landslide deformation behavior influenced by water level fluctuations of the Three Gorges Reservoir (China). Eng Geol 247:58–68

Sun G, Yang Y, Jiang W, Zheng H (2017) Effects of an increase in reservoir drawdown rate on bank slope stability: a case study at the Three Gorges Reservoir, China. Eng Geol 221:61–69

Tang H, Wasowski J, Juang CH (2019) Geohazards in the three Gorges Reservoir Area, China—lessons learned from decades of research. Eng Geol 261:105267

Tomás R, Li Z, Lopez-Sanchez JM, Liu P, Singleton A (2016) Using wavelet tools to analyse seasonal variations from InSAR time-series data: a case study of the Huangtupo landslide. Landslides 13(3):437–450

Udvardi B, Kovács IJ, Szabó C, Falus G, Újvári G, Besnyi A, Bertalan É (2016) Origin and weathering of landslide material in a loess area: a geochemical study of the Kulcs landslide, Hungary. Environ Earth Sci 75(19):1299

Wang JE, Xiang W, Lu N (2014) Landsliding triggered by reservoir operation: a general conceptual model with a case study at Three Gorges Reservoir. Acta Geotech 9(5):771–788

Wen BP, Wang SJ, Wang EZ, Zhang JM (2004) Characteristics of rapid giant landslides in China. Landslides 1:247–261

Wen BP, Aydin A, Duzgoren-Aydin NS, Li YR, Chen HY, Xiao SD (2007) Residual strength of slip zones of large landslides in the Three Gorges area, China. Eng Geol 93:82–98

Wolter A, Stead D, Ward BC, Clague JJ, Ghirotti M (2016) Engineering geomorphological characterisation of the Vajont slide, Italy, and a new interpretation of the chronology and evolution of the landslide. Landslides 13(5):1067–1081

Wu Y, Miao F, Li L, Xie Y, Chang B (2017) Time-varying reliability analysis of Huangtupo Riverside No. 2 Landslide in the Three Gorges Reservoir based on water-soil coupling. Eng Geol 226:267–276

Xu Q, Tang MG, Xu KX, Huang XB (2008) Research on space-time evolution laws and early warning-prediction of landslides. Chin J Rock Mech Eng 27(6):1104–1112 (in Chinese)

Yin YP, Huang B, Chen X, Liu G, Wang S (2015) Numerical analysis on wave generated by the Qianjiangping landslide in Three Gorges Reservoir, China. Landslides 12:355–364

Zhang Z, Wang D, Wang L, Huang R, Xu Q (1994) Engineering geology analysis principle. Geology Publishing House, Beijing, pp 184–231

Zhang J, Zhang LM, Tang WH (2011) New methods for system reliability analysis of soil slopes. Can Geotech J 48(7):1138–1148

Zhang ZH, Jiang QH, Zhou CB, Liu XT (2014) Strength and failure characteristics of Jurassic red-bed sandstone under cyclic wetting-drying conditions. Geophys J Int 198(2):1034–1044

Zhang BY, Zhang JH, Sun GL (2015) Deformation and shear strength of rockfill materials composed of soft siltstones subjected to stress, cyclical drying/wetting and temperature variations. Eng Geol 190:87–97

Zhang Y, Hu X, Tannant DD, Zhang G, Tan F (2018) Field monitoring and deformation characteristics of a landslide with piles in the three gorges reservoir area. Landslides 15(3):581–592

Zhu H, Zhang LM, Zhang L, Zhou C (2013) Two-dimensional probabilistic infiltration analysis with a spatially varying permeability function. Comput Geotech 48:249–259

K. Liao · Y. Wu (✉) · F. Miao · L. Li · Y. Xue
Faculty of Engineering,
China University of Geosciences,
Wuhan, 430074, China
Email: ypwu@cug.edu.cn

L. Li
e-mail: linweili93@126.com

Y. Xue
e-mail: egxyang@163.com